Technical University of Denmark

DTU

Implementation of Synthetic Aperture Imaging in Medical Ultrasound
The Dual Stage Beamformer Approach

Jensen, Jørgen Arendt; Kortbek, Jacob; Nikolov, Svetoslav; Hemmsen, Martin Christian; Tomov, Borislav Gueorguiev

Publication date:
2010

Document Version
Publisher's PDF, also known as Version of record

Link back to DTU Orbit

DTU Library
Technical Information Center of Denmark

Implementation of Synthetic Aperture Imaging in Medical Ultrasound: The Dual Stage Beamformer Approach

Jørgen Arendt Jensen[1], Jacob Kortbek[2], Svetoslav I. Nikolov[2], Martin Hemmsen[1,2] and Borislav Tomov[1]

[1]Department of Electrical Engineering, Center for Fast Ultrasound Imaging, Build. 349,
Technical University of Denmark, DK-2800 Lyngby, Denmark
[2]B-K Medical, Mileparken 34, 2730 Herlev, Denmark

Abstract

The main advantage of medical ultrasound imaging is its real time capability, which makes it possible to visualize dynamic structures in the human body. Real time synthetic aperture imaging puts very high demands on the hardware, which currently cannot be met. A method for reducing the number of calculations and still retain the many advantages of SA imaging is described. It consists of a dual stage beamformer, where the first can be a simple fixed focus analog beamformer and the second an ordinary digital ultrasound beamformer. The performance and constrictions of the approach is described.

1 Introduction

In medical ultrasound simple delay-and-sum beamforming is traditionally used. Here a single fixed transmit focus is employed. The received signals are digitized and beamformed in a digital beamformer with dynamic receive focusing and dynamic Hanning or Gauss apodization, where more elements are included for larger depths. Usually 64 to 128 active elements are used in transducers with a center frequency of 5-12 MHz and a 100% bandwidth. A Full-Width-Half-Max (FWHM) resolution of 1-2 λ is obtained axially and around 1 λ laterally with side-lobes being attenuated more then 60 dB. The transducer pitch is 2 - 3 λ for linear array transducers used in rectangular sized scans and λ for phased array transducers used in polar scans. The large dynamic range demands very tight control over the transducer geometry and the beamforming done where the focusing delays change dynamically with depth.

A requirement in medical ultrasound is that imaging is real time, so that the dynamic function of organs and views form different directions can be seen. More than 20 frames should be shown per second and in cardiac imaging often 50-60 frames per second is sought achieved. This puts a heavy demand on the processing hardware that often have to process 5 - 10 Gbytes of data per second in a system that must be transportable by one person.

The major drawback of current systems is that there is only one transmit focus and that the imaging is sequential. This limits image quality and the frame rate is limited by the speed of sound (1540 m/s in the human body). This is especially a problem in 3D imaging, where many directions have to be probed. The acquisition of data for velocity estimation is also difficult, since data have to be measured in the same direction several times, thus, lowering the frame rate. Other more efficient and high quality methods for data acquisition are, thus, needed.

2 Synthetic aperture ultrasound imaging

Synthetic aperture data acquisition can be used in medical ultrasound imaging as has been shown by a number of authors. The method can either be employed for single element or multi-element transducers. Many variations of synthetic aperture focusing (SAF) and examples of implementation have been reported with improvements in both frame rate, penetration, and lateral resolution. This includes single channel system [1, 2], where the same element serves as a transmitter and a receiver. Systems with multi-element transmit and receive aperture was described by Karaman et al. [3] and Lockwood and Hazard [4, 5]. A SA method for a circular aperture was investigated by O'Donnell and Thomas [6].

A typical method for acquiring the data is shown in Fig. 1, where the transmit focusing is synthesized. A single or a few elements are combined to send out a spherical wave to insonify the whole region of interest. The scattered signal is then received by some or all of elements in the transducer. A low resolution image can be formed after each transmit event by summing the signals from all receiving elements as

$$y_{lr}(\vec{r}_p, j) = \sum_{i=1}^{N_{ele}} a(i,j) g_i(t_d(i,j), j)$$

where $\vec{r}_p$ is the point in the image, N_{ele} is the number of receive elements, $a(i,j)$ is the apodization or relative weight of the signal $g_i(t)$ from the received element signal for element i and j is the transmission number. The time point t_d at which the signal value is taken is calculated from the geometric distance between transmit position $\vec{r}_t(j)$, the image point and the receiver location $\vec{r}_r(i)$ as

$$t_d(i,j) = \frac{|\vec{r}_p - \vec{r}_t(j)| + |\vec{r}_p - \vec{r}_r(i)|}{c}.$$

The process is then repeated for the next transmit element to cover all elements as transmitters in the transducer. All low resolution images are summed, and this yield a high resolution image, which is both dynamically focused in transmit and receive resulting from the precise calculation of the delay $t_d(i, j)$.
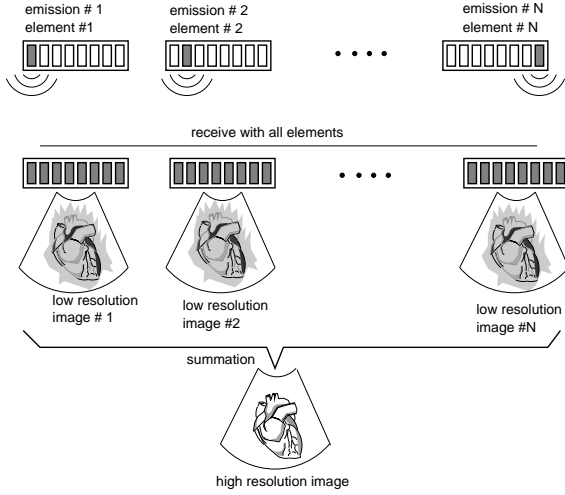

Figure 1: Data acquisition in synthetic aperture imaging (from [7].)

The method ensures an optimal resolution and side-lobe levels for the delay-and-sum beamformer for the particular transducer. It can also be combined with a sparse transmit sequence to make fast imaging or make it suitable for SA flow imaging [8].

The major drawback of the approach is the large number of calculations to be performed. A full new low-resolution image must be made each time a new pulse is emitted. The number of complex beamformed samples per second is

$$N_{bs} = N_{ele}N_lN_sf_{prf},$$

where N_l is the number of lines in an image (100-200), N_s is the number of samples (500-1000), and f_{prf} is the pulse repetition frequency (10 kHz at 7.5 cm depth of scanning, 5 kHz 15 cm). A normal scan situation at 7.5 cm for 192 channel array would yield $38.4 \cdot 10^9$ complex samples per second for 200×1000 images with substantial data rates also. For all of these data the delay t_d have to be calculated as well as interpolating data and apodizing them. This has precluded the introduction of commercial SA scanner so far. More efficient techniques are, thus, needed.

3 Dual stage beamforming

The major problem in SA imaging is that a low resolution images are formed after each emission and that there are data from many receive channels. The dual-stage beamforming approach presented here is a compromise between image quality and the possibility of implementing SA imaging on a simple platform [9, 10].

The implementation consists of two parts: a simple fixed focus receive beamformer followed by a traditional digital beamformer capable of dynamic delay-and-sum beamforming. The first beamformer emits a beam focused close to the transducer and receive the scattered signal by a number of elements. The F-number ($F\#$ =depth/aperture width) is fairly low around 1-2 and keeping the depth low ensures that only a modest amount of elements have to be used. The number of transmitting and receiving channels are, thus, low and a simple analog, fixed delay beamformer can even be used for keeping price down. The second stage beamformer receives the data from the first and combines a number of emissions to dynamically focus the data in both transmit and receive. The time delay t_d is here calculated from the travel time from the emission focus to the imaging point and back to the transducer. Several approach based on a virtual source [11, 12, 13, 14] can be used and they are described in more detail in [9, 10].

The digital beamformer can yield one new high resolution line each time it receives a signal from the first beamformer and the demands are, thus, not higher than for an ordinary digital beamformer if the emission line density and the final image line density are the same. More calculations have to be performed if the final line density is higher, but often high end beamformers can produce 4 to 16 beamformed signals per emission. This feature can also be used to cover more emissions. The limitation is that the number of first stage beamformed lines is restricted by the number of input channels to the beamformer, but it is possible to combine two beamformed lines by adding them. Hereby twice the number of emissions can be used for one high resolution line at the price of a reduction in output data rate.

The approach is, thus, flexible and can be readily implemented in commercial scanners with minimal modification of the hardware. Actually the number of active receive channels, which are the most expensive in a scanner, can be reduced to one, if a suitable analog beamformer is used in the first stage. The method can therefore be used in both low-end as well as high-end scanner and still maintain a good image quality.

4 Results

The method has been investigated using both the Field II simulation program [15, 16] and measurements on phantom objects.

A 191 elements linear array transducer with a center frequency of 7 MHz, relative bandwidth of 0.6, pitch of 0.208 mm, and an elevation focus of 25 mm has been used. Imaging with synthetic aperture sequential beamforming (SASB) is compared to normal dynamic receive focusing (DRF) in Fig. 2, where the transmit focus was set at 70 mm. For SASB imaging $F\# = 1.5$ and the transmit focus was at 20 mm, so that the transducer uses 64 elements in transmit. It can be seen that the point targets maintain

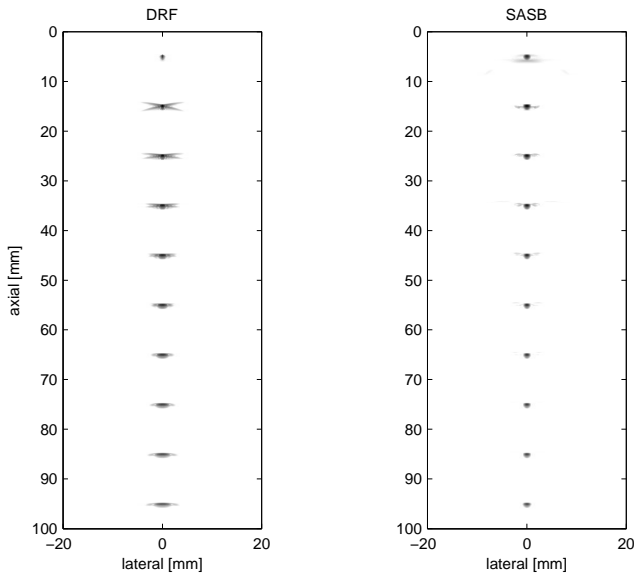a more uniform and narrower appearance throughout the depth compared to DRF.

Figure 2: Envelope images using DRF (left) and SASB (right). For DRF the transmit focal point is at 70 mm. For SA the VS is at 20 mm and $F\# = 1.5$. Dynamic Range is 60 dB (from [10]).

The performance can be quantified for the -6 dB and -40 dB resolution. This is given in Fig. 3, where the performance is compared for different transmit foci and different number of receive elements in the second-stage beamformer. The SASB method maintains its narrow focusing for nearly all depths and is apart from the very near field always better than DRF.

A measurement has also been performed on a tissue mimicking phantom using a BK Medical ProFocus scanner equipped with a research interface. The scanner then mimics the first stage beamformer and data are stored for post-processing for emulating the second stage beamformer. The various images are shown Fig. 4. The left images show the data right after the first stage beamformer, the middle image shows the SASB image and the right panel shows the conventional ultrasound image. Again a clear difference and improvement can be seen. A further advantage of SASB is that the signal-to-noise ratio is improved in the images and imaging to greater depths can be attained [10].
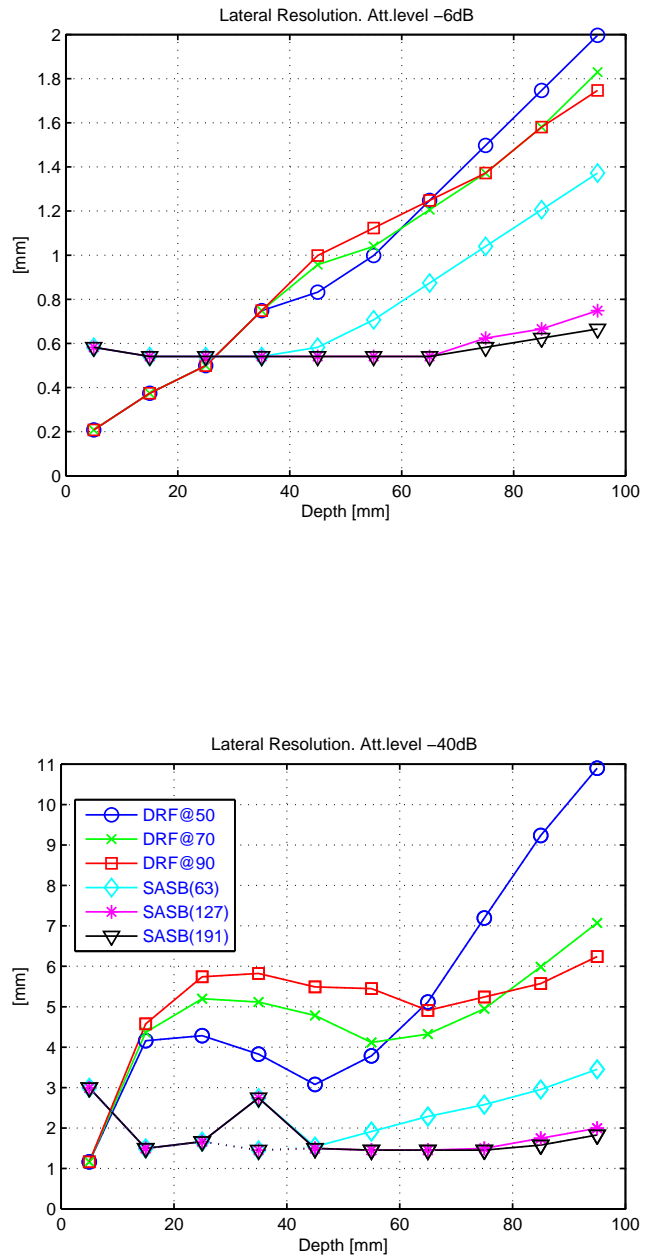

Figure 3: Lateral resolution of DRF and SASB as function of depth at -6 dB (top) and -40 dB (bottom). If the lateral PSF has a distinct main-lobe, and side-lobe distribution, the main-lobe resolution is shown as a dotted line. For DRF the transmit focal point is at 50 mm, 70 mm, and 90 mm. For SASB the VS is at 20 mm and $F\# = 1.5$. SASB results are presented using different number of available 2nd stage beamformer channels ($N_{2nd} = 63$, $N_{2nd} = 127$, and $N_{2nd} = 191$), (from [10]).
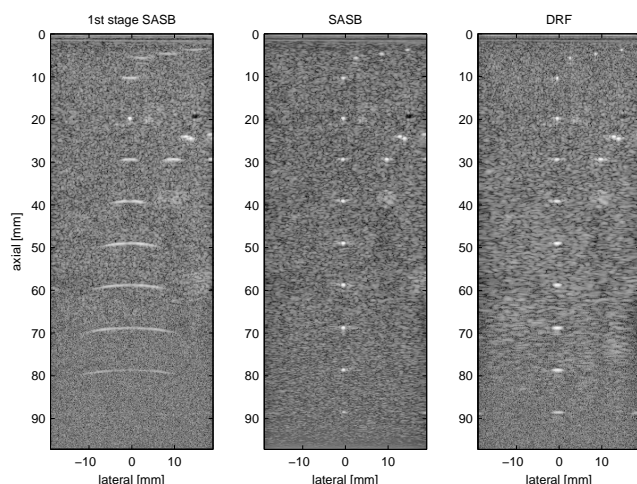
Figure 4: Envelope images using 1st stage SASB (left), SASB (center), and DRF (right). RF-data is acquired using a commercial scanner, and processing is done off-line. For DRF the transmit focal point is at 65 mm. For SASB the VS is at 20 mm and $F\# = 2$. Dynamic Range is 60 dB (from [10]).

5 Conclusion

A method for reducing the complexity of synthetic aperture imaging has been suggested. By implementing SA in two stages with a simple beamformer first many of the advantages of SA imaging can be attained without the need for a large number of calculations. Using simulations and phantom measurements it was shown that the resolution, contrast, and penetration depth is improved compared to normal dynamic delay-and-sum beamforming employed in modern ultrasound scanners.

References

[1] D. K. Peterson and G. S. Kino. Real-time digital image reconstruction: A description of imaging hardware and an analysis of quantization errors. *IEEE Trans. Son. Ultrasound.*, 31:337–351, 1984.

[2] J. T. Ylitalo and H. Ermert. Ultrasound synthetic aperture imaging: monostatic approach. *IEEE Trans. Ultrason., Ferroelec., Freq. Contr.*, 41:333–339, 1994.

[3] M. Karaman, P. C. Li, and M. O'Donnell. Synthetic aperture imaging for small scale systems. *IEEE Trans. Ultrason., Ferroelec., Freq. Contr.*, 42:429–442, 1995.

[4] G. R. Lockwood, J. R. Talman, and S. S. Brunke. Real-time 3-D ultrasound imaging using sparse synthetic aperture beamforming. *IEEE Trans. Ultrason., Ferroelec., Freq. Contr.*, 45:980–988, 1998.

[5] C. R. Hazard and G. R. Lockwood. Theoretical assessment of a synthetic aperture beamformer for real-time 3-D imaging. *IEEE Trans. Ultrason., Ferroelec., Freq. Contr.*, 46:972–980, 1999.

[6] M. O'Donnell and L. J. Thomas. Efficient synthetic aperture imaging from a circular aperture with possible application to catheter-based imaging. *IEEE Trans. Ultrason., Ferroelec., Freq. Contr.*, 39:366–380, 1992.

[7] S. I. Nikolov. *Synthetic Aperture Tissue and Flow Ultrasound Imaging.* PhD thesis, Ørsted•DTU, Technical University of Denmark, 2800, Lyngby, Denmark, 2001.

[8] S. I. Nikolov and J. A. Jensen. In-vivo Synthetic Aperture Flow Imaging in Medical Ultrasound. *IEEE Trans. Ultrason., Ferroelec., Freq. Contr.*, 50(7):848–856, 2003.

[9] J. Kortbek, J. A. Jensen, and K. L. Gammelmark. Synthetic aperture sequential beamforming. In *Proc. IEEE Ultrason. Symp.*, pages 966–969, 2008.

[10] J. Kortbek, J. A. Jensen, and K. L. Gammelmark. Synthetic aperture sequential beamforming. *J. Acoust. Soc. Am.*, page Submitted, 2009.

[11] C. Passmann and H. Ermert. A 100-MHz ultrasound imaging system for dermatologic and ophthalmologic diagnostics. *IEEE Trans. Ultrason., Ferroelec., Freq. Contr.*, 43:545–552, 1996.

[12] C. H. Frazier and W. D. O'Brien. Synthetic aperture techniques with a virtual source element. *IEEE Trans. Ultrason., Ferroelec., Freq. Contr.*, 45:196–207, 1998.

[13] M. H. Bae and M. K. Jeong. A study of synthetic-aperture imaging with virtual source elements in B-mode ultrasound imaging systems. In *IEEE Trans. Ultrason., Ferroelec., Freq. Contr.*, volume 47, pages 1510–1519, 2000.

[14] S. I. Nikolov and J. A. Jensen. Virtual ultrasound sources in high-resolution ultrasound imaging. In *Proc. SPIE - Progress in biomedical optics and imaging*, volume 3, pages 395–405, 2002.

[15] J. A. Jensen and N. B. Svendsen. Calculation of Pressure Fields from Arbitrarily Shaped, Apodized, and Excited Ultrasound Transducers. *IEEE Trans. Ultrason., Ferroelec., Freq. Contr.*, 39:262–267, 1992.

[16] J. A. Jensen. Field: A Program for Simulating Ultrasound Systems. *Med. Biol. Eng. Comp.*, 10th Nordic-Baltic Conference on Biomedical Imaging, Vol. 4, Supplement 1, Part 1:351–353, 1996b.